Analysis of Pattern Distortion by Panel Deformation and Addressing it by Using Extremely Large Exposure Field Fine-Resolution Lithography

John Chang[1], Corey Shay[2], James Webb[3], Timothy Chang[4]
Onto Innovation Inc.
Massachusetts 01887, USA
[1]John.Chang@ontoinnovation.com, [2]Corey.Shay@ontoinnovation.com, [3]James.Webb@ontoinnovation.com,
[4]Timothy.Chang@ontoinnovation.com

***Abstract*— The growing demand for heterogeneous integration is driven by the 5G market. This includes smartphones, data centers, servers, high-performance computing (HPC), artificial intelligence (AI) and internet of things (IoT) applications. Next-generation packaging technologies require tighter overlay to accommodate larger package sizes with fine-pitch chip interconnects on large-format flexible panels. Heterogeneous integration enables device performance gains by combining multiple silicon nodes and designs inside one package. The package size is expected to grow significantly, increasing to 75mm x 75mm and 150mm x 150mm, within the next few years. For these requirements, an extremely large exposure field fine-resolution lithography solution was proposed to enable packages well over 250mm x 250mm without the need for image stitching, while exceeding the overlay and critical uniformity requirements for these packages.**

One of the challenges of extremely large exposure field fine-resolution lithography is to achieve an aggressive overlay number. Formation changes experienced by the panel as a result of thermo, high-pressure and other fan-out processes shift the design location from nominal coordinates; this causes inaccurate overlay and low-overlay yield in the lithography process. Addressing this critical lithography challenge becomes an important task in heterogeneous integration.

In this paper, a 515mm x 510mm Ajinomoto build-up film (ABF)+copper clad laminate (CCL) substrate is selected as the test vehicle. We will analyze the pattern distortion of an ABF+CCL substrate to understand the distribution of translation, rotation, scale, magnification, trap, orthogonality and other errors in the substrate, and then use extremely large exposure field fine-resolution lithography to address the pattern distortion of the substrate. This demonstration will provide an analysis of panel distortion and detail how the extremely large exposure field fine-resolution lithography solution addresses panel distortion to achieve an aggressive overlay number.

Keywords: 5G, HPC, AI, IoT, Heterogeneous Integration (HI), Advanced IC Substrate (AICS), Advanced Packaging (AP), OSAT, Fan-out Panel-level Packaging (FOPLP), Overlay, Distortion, Large Exposure Field, Fine Resolution.

I. INTRODUCTION

Heterogeneous integration requires the integration of multiple chips into a single 75mm x 75mm or 150mm x 150mm package for increased functionality. These large packages will be a new challenge for manufacturing processes. For current advanced packaging lithography steppers, processing such large package sizes requires the use of multiple exposure shots to complete a package because of the limitation of the exposure field size. This method, known as "stitching," requires multiple reticles and has low throughput, which increases costs. However, increasing the stepper field size removes the need for stitching and increases throughput significantly.

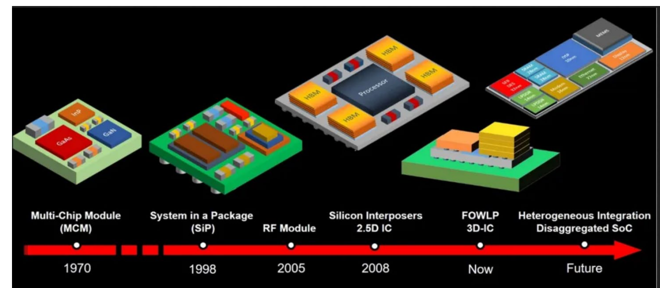

Fig 1. Heterogeneous integration enables next-generation device performance gains by combining multiple silicon nodes and designs inside one package, so the package size is expected to grow significantly. (Source: Cadence)

The extremely large (250mm x 250mm) exposure field allows the user to process one or more large packages in a single shot and requires less shots to complete a substrate. This offers a significant throughput increase over regular exposure fields. However, there are significant process challenges, such as panel warpage and deformation changes during the build-up of multi-RDL layers; these process challenges impact critical dimension and overlay control. Fig 2 shows the exposure layout of an extremely large exposure field (250mm x 250mm) and a regular exposure field (59mm x 59mm) on a 510mm x 515mm panel. With the extremely large exposure field, a panel can be completed with just four (4) shots; with a regular exposure field, a panel requires 64 shots to complete.

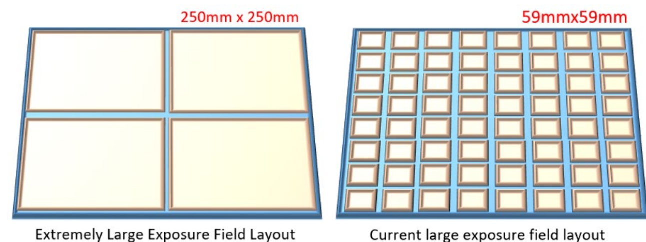

Fig 2. The 510mm x 515mm panel exposure layout comparison. The left figure is an example exposure layout of an extremely large exposure field; the right figure is an example exposure layout of a regular exposure field. The

onto innovation

extremely large exposure field uses less shots to complete a panel and enables larger packaging sizes.

Overlay is one of the major challenges in the HI packaging build-up process. During the packaging build-up processes, multi-RDL layers will be added. These processes may cause various stresses on the surface or inside the substrate and may then cause substrate warpage and formation change. Substrate warpage or formation change causes known good die (KGD), core pattern or alignment mark shift from its nominal position. In panel-level packaging, this situation is more serious; if left uncorrected during the exposing process, these factors can result in serious overlay errors.

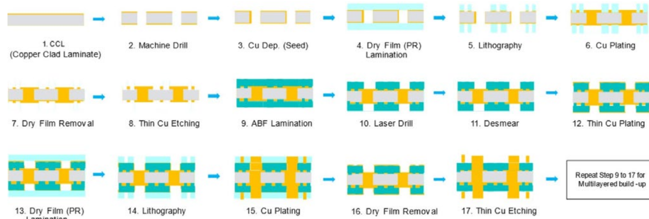

Fig 3. A typical IC substrate packaging build-up process flow: During RDL layer build-up process, the substrate suffered deformation from high stress, high temperature and other process steps; the substrate deformation induces a pattern shift from the nominal position and affects the overlay results in the lithography process.

In this study, we will demonstrate the performance of an extremely large exposure field fine-resolution lithography system to understand its resolution, overlay and correction capabilities. For the purpose of this study, a 510mm x 515mm panel with RDL layers stacked on CCL substrate was selected as a test vehicle. In this paper we will discuss how we used metrology data from the lithography system, combined with overlay analysis algorithms, to identify the error terms and distortion components of the test vehicle and find a solution / strategy to correct the errors. The test vehicle was exposed with an extremely large exposure field fine-resolution system. After using the solution / strategy to correct the errors and distortion, we reviewed the overlay results to verify if the proposed correction solution fixes the errors and distortion. In the final section of this study, we will discuss overlay results and overlay yield improvement.

II. Experiment Details

A. Test Vehicle and Exposure Layout

In order to demonstrate the capabilities of an extremely large exposure filed fine-resolution lithography system, we selected 510mm x 515mm glass panels with stacked CCL+ABF panels as the test vehicles. For panel error terms and distortion analysis and overlay demonstration, we selected 510mm x 515mm core board panels with stacked CCL+ABF panels. With exposure shots at 250mm x 250mm a shot, we exposed the panel in four (4) shots.

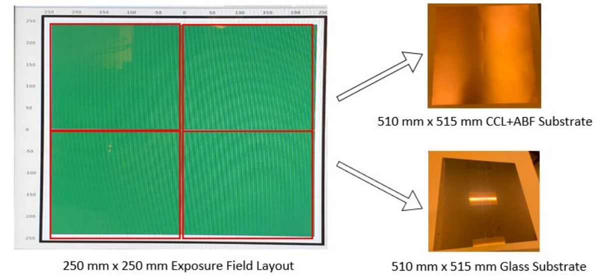

Fig 4. Exposure layout with four (4) 250mm x 250mm exposure field shots, four (4) shots on 510mm x 515mm CCL+ABF substrate and 510mm x 515mm glass substrate.

B. Extremely Large Exposure Field Fine Resolution Lithography

The extremely large exposure field fine-resolution lithography system employed in this study is a JetStep® X500 system (Onto Innovation). This system supports 510mm x 515mm glass panels and CCL substrates. The system is equipped with a 2.2x magnification projection lens, which enables up to a 250mm x 250mm exposure field size, with 3µm line/space resolution, ±400ppm magnification compensation and ±100ppm anamorphic magnification compensation, with an overlay of < 1µm. Critical dimension and overlay are the keys to achieving practicable lithography; when using an extremely large exposure field system, how to achieve these requirements must be taken into consideration.

- **Resolution Performance of ELEF Lithography**

In order to demonstrate the resolution performance of the lithography system, a CCL+ABF substrate with 10µm-thick dry film resist was selected, and the substrate was exposed during four (4) 250mm x 250mm shots, resulting in a complete exposure. Fig 5 shows the resolution demonstration results; 3µm line / space can be well resolved, and the depth of focus is up to 60µm.

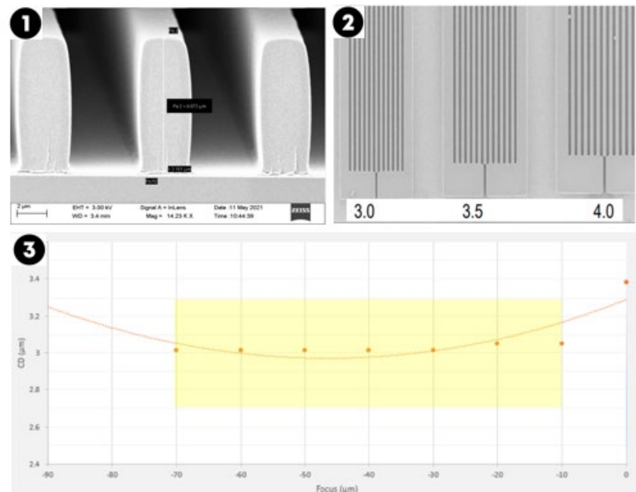

onto innovation

Fig 5. Extremely large exposure field fine-resolution lithography system resolution performance: ① Cross section image of 3µm line / space with 10µm thick dry film resist, which is 1:3.3 aspect ratio. ② Isolated and dense area resolution results of 3µm, 3.5µm and 4µm line/space. ③ Bossung curve of 3µm L/S with a 10µm-thick dry film resist. The X axis is focus (µm), and the Y axis is CD (µm). A 60µm depth of focus is observed in 3µm line / space with 10µm-thick dry film resist.

- **Overlay Performance of ELEF Lithography**

To demostrate the overlay performance of the lithography system, a 510mm x 515mm glass panel with 1.4µm liquid resist was selected as a test vehicle. The first layer was built on the test panel. The entire layout of the first layer was exposed by a total of four (4) shots, with an exposure field of 250mm x 250mm per shot. The test vehicle is run with a site-by-site correction method at four (4) shots per panel to build the second layer. We then checked the overlay error between layer 1 and layer 2 to determine the overlay performance. The overlay error was determined by reading the overlapped verniers in certain locations. Each exposure field contains 3 x 3 measurement points, and 2 x 2 shots a panel were measured to determine the overlay performance of the lithography system. Fig 6 shows the overlay results of the extremely large exposure field lithography system.

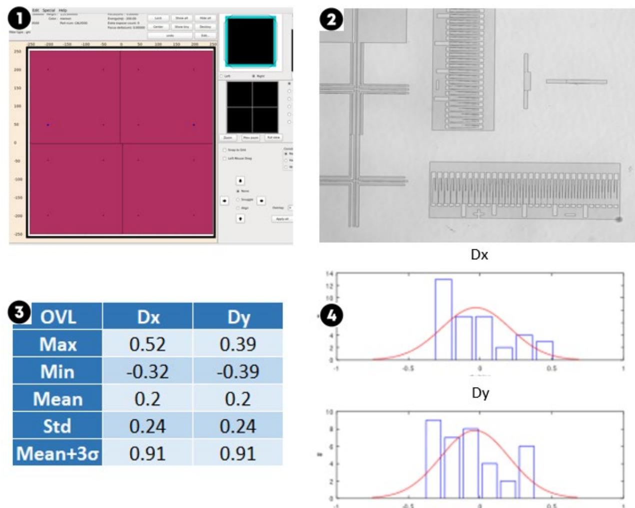

OVL	Dx	Dy
Max	0.52	0.39
Min	-0.32	-0.39
Mean	0.2	0.2
Std	0.24	0.24
Mean+3σ	0.91	0.91

Fig 6. The overlay performance of the extremely large exposure field fine-resolution lithography system: ① Exposure layout for overlay demonstration, with four (4) shots per panel at 250mm x 250mm a shot. ② Overlapped verniers built by the first layer and second layer: the overlay performance was determined by reading the verniers. ③ Overlay statistics table: The deviation X mean +3 sigma is 0.91µm, and the deviation Y mean +3 sigma is 0.91µm. These numbers indicate an extremely large exposure field fine-resolution lithography system can achieve an aggressive overlay number less than 1µm. ④ Dx and Dy distribution chart: the mean is close to center, and no peak distribution is observed.

- **Overlay Correction Capability**

The lithography system was combined with intra-field correction capability and global correction capability to correct the errors on the substrate. Fig 7 shows the overlay corrective capability of the extremely large exposure field fine-resolution lithography system. Translation, rotation, scale and orthogonality correction are available in global correction; translation, rotation, magnification, radial distortion and trapezoid correction are available in intra-field correction. Anamorphic magnification and skew corrections are available with combined global correction and intra-field correction.

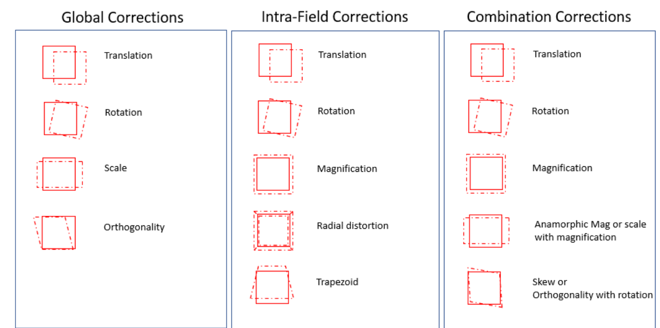

Fig 7. Extremely large exposure lithography fine-resolution system corrections. The left figure is of global corrections, included translation, rotation and scale and orthogonality. The middle figure is of intra-field corrections, including translation, rotation, magnification, radial distortion and trapezoid. The right figure is of overlay corrections combined with global and intra-field ability, which included translation, rotation magnification, anamorphic magnification and skew.

C. Test Vehicle Distortion Components and Analysis

We selected CCL+ABF panels, stacked with core pattern substrates, measuring 510mm x 515mm, for error terms and distortion components analysis. In this study, the lithography system was used for collecting the metrology data of the test vehicles. The lithography system equips RAS (reflective alignment system) and grid stage; RAS can recognize the alignment mark on the substrate. Combined with grid stage information, the pattern deviation of the substrate can be identified and collected.

The analysis in this study uses metrology data generated by the lithography system combined with the following algorithms: Steppermatch® (Onto Innovation's propriety algorithm) and Dolana. Based on the field-size capabilities of an extremely large exposure field fine-resolution lithography system, the 510mm x 515mm panel was exposed in four shots, at 250mm x 250mm per shot. These four shots were analyzed for error terms and distortion components.

- **The Error Terms and Distortion Components of Test Vehicle**

With metrology data collected by the lithography system and analyzed by the Donala algorithm, the error terms and distortions in the test vehicles were identified. Anamorphic pincushion and third radial distortion can be observed when describing errors in a full-panel model; however, the error terms change when observed in a quadrant of the panel (lens field). The error terms change to include translation, magnification, anamorphic magnification, rotation, skew and trapezoid. Fig 8 shows the error terms and distortion components in a quadrant of the panel, and Fig 9 shows the error terms in a full-panel model.

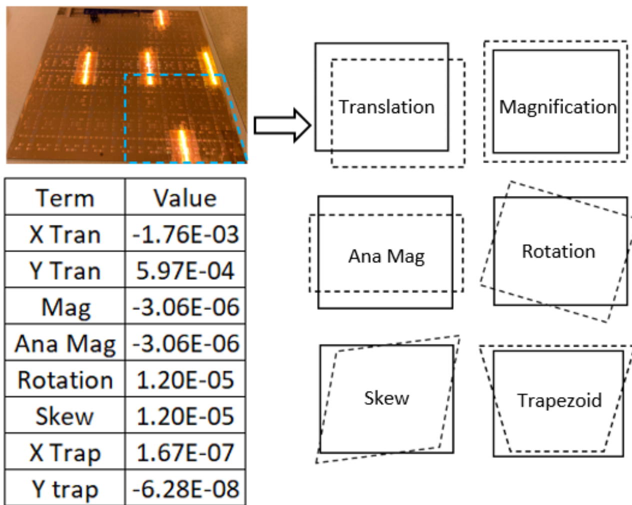

Term	Value
X Tran	-1.76E-03
Y Tran	5.97E-04
Mag	-3.06E-06
Ana Mag	-3.06E-06
Rotation	1.20E-05
Skew	1.20E-05
X Trap	1.67E-07
Y trap	-6.28E-08

Fig 8. Error terms and distortion components are identified in a quadrant of a 510 mm x 515 mm test vehicle. The numbers in the table are the coefficients used in the equations of the algorithm that describe each term fit.

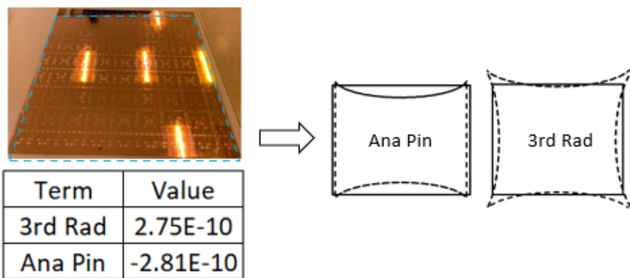

Term	Value
3rd Rad	2.75E-10
Ana Pin	-2.81E-10

Fig 9. Anamorphic pincushion and third radial distortion can be observed in the full-panel model. The numbers in the table are the coefficients used in the equations of the algorithm that describe each term fit.

- **Global Solution Correction vs. Zone Solution Correction**

Various error terms and distortion signatures were found for each quadrant of the 510mm x 515mm panel. This indicates that global solution correction cannot fully correct test vehicle error and distortion. A unique correction is needed for each quadrant to correct the unique errors during exposure; by doing this, we were able to achieve good overlay results. Fig 10 shows error vector maps for global solution corrections and zone solution corrections; these two error vector maps are from the same test vehicle. According to the error vector maps, global solution translation corrections show that translation errors vector toward the down-left direction, but in the bottom-right quadrant of the zone correction solution, the translation error vectors toward the upper-right direction, which is the opposite direction of the global solution correction. Other correction components can be observed in different directions or trends in each quadrant.

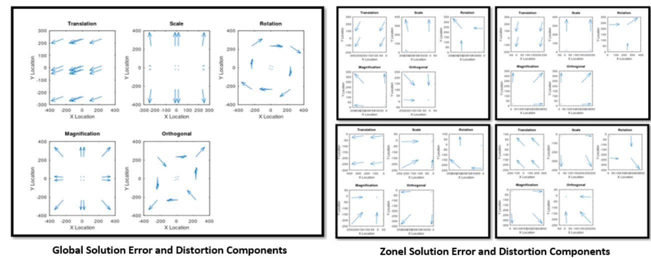

Fig 10. Global solution correction vs. zone solution correction. Various distortion trends can be observed in each quadrant. Zone solution correction can be expected to reach better overlay numbers compared with global solution correction.

D. *Overlay Results and Analysis*

The test vehicle was processed with liquid film. Using the lithography system, combined with a proprietary algorithm, corrections were generated for each quadrant of the test vehicle. The corrections were used during exposure, and then the test vehicle was taken to development. Overlay measurements were taken by optical microscope using measurement software, with six (6) measuring points per zone, four (4) zones per panel, totaling 24 measuring points per sampling. Four (4) measuring points were at the four (4) corners, the top-right, top-left, bottom-right and bottom left corners. Two (2) measuring points were at the center of the zone. These measuring points were used to verify the overlay results of the entire area of the test vehicle. Fig 11 describes how the overlay deviation X, deviation Y and vector were defined.

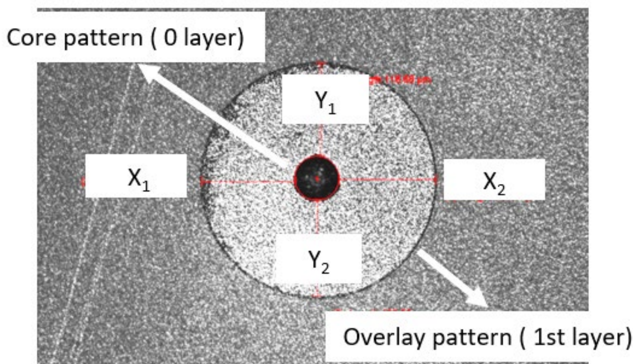

Fig 11. Overlay measuring method to determine the overlay dx, dy and vector. Center black spot is core pattern, the bigger circle is of the overlay pattern, $dx = X_1 - X_2$, $dy = Y_1 - Y_2$ and error vector $= \sqrt{(dx^2+dy^2)}$.

Fig 12 shows the overlay results of the test vehicle. The deviation X maximum is 5.42µm and shifts right; the deviation Y maximum is 5.72µm and shifts upward. Based on the substrate provider database, if the distortions and errors are recognized well and corrected properly, the final overlay error can be expected to be less than 10µm. Fig 12 shows the final overlay error vector results are less than 7µm, and dx and dy values are within ±6µm. This indicates that the errors and distortions of the test vehicle are recognized correctly and corrected as expected, but if the errors and distortions are not corrected properly, the overlay error vector could be up to 20µm or higher (Fig 13).

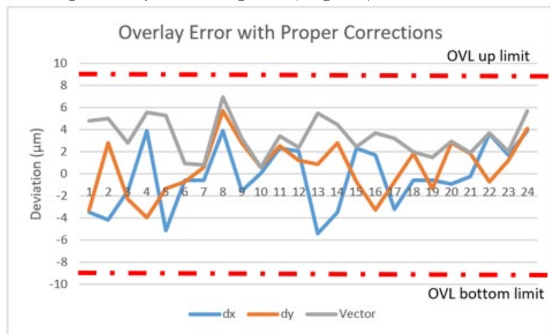

	Dx	Dy	Vector
Max	3.94	5.72	6.94
Min	-5.42	-3.94	0.58
Average	-0.24	0.57	3.37
STD	2.89	2.47	1.74

Unit : µm

Fig 12. Test overlay results with proper corrections and method. With the zone solution correction method and proper corrections, which included translation, rotation, magnification, anamorphic magnification, skew and orthogonality corrections, the final overlay results reach a range of ±6µm.

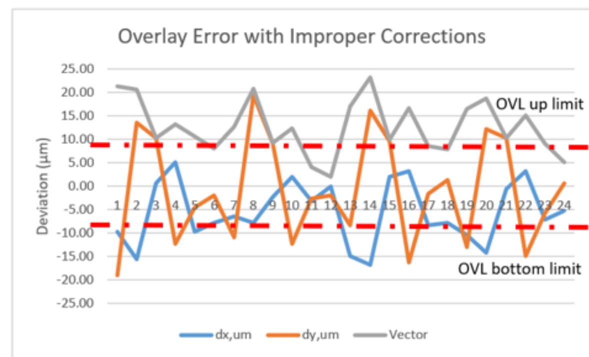

	Dx	Dy	Vector
Max	5.16	19.35	23.26
Min	-16.77	-19.06	1.94
Average	-5.47	-0.95	12.67
STD	6.46	11.26	5.76

Unit : µm

Fig 13. Overlay results using improper corrections and method. Without zone solution correction, the overlay error was up to ±20µm in the X and Y axis, the overlay vector was up to 23.26µm. These numbers indicate that improper corrections and method were applied during exposure resulting in poor overlay.

III. ANALYSIS AND DISCUSSION

According to an analysis of error terms and distortion components, translation, rotation, scale, magnification, anamorphic magnification, skew, trapezoid and orthogonality errors were observed in the test vehicle. These errors needed to be corrected by a lithography tool to achieve better overlay results. Various trending errors and distortion signatures also were observed in each quadrant of the 510mm x 515mm panel. Observations indicate that zone solution correction should be applied during exposure to enable better overlay results. The analysis indicates that a reasonable overlay results can be achieved by using proper corrections and zone solution corrections, but even with using proper corrections and zone solution correction method, we still see a 7um overlay residual error. We would like to understand what induce this residual error.

- **Fake Alignment Solution**

According to analysis of the test vehicles and the panel build process, we found out this residual error could be induced by "fake alignment solution", the fake alignment solution make a "unreal position information" to system, and it leads the system generate incorrect corrections to compensate the error and distortion on the panel, then results the overlay shift. The possible factors of fake alignment solution are identified as poor contract alignment mark, poor shape of the alignment mark, laser driller position error and irregular panel deformation, the first two factors make system cannot recognize the center of mark accurate, the rest of the factors make the alignment mark position shift from where it should be. Fig 14 is an example of poor alignment marks shape.

innovation onto

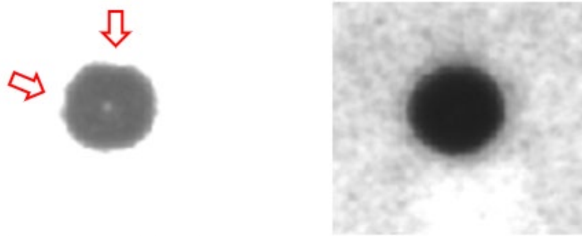

Fig 14. Alignment mark by laser drill system. The left figure has a poor shape compared to the right figure. This situation could result in alignment solution errors and affect final overlay. Alignment marks could contain one or multiple laser marks.

- **Additional Compensation Improves Overlay**

To address fake alignment solution issue and improve overlay in advance, additional compensation is proposed. A proprietary algorithm was used for predicting the overlay results with additional compensation. The algorithm was used for analyzing the correctable terms based on current overlay errors, such as translation, rotation, scale, magnification and orthogonality; predictions regarding the final overlay results, following the removal of correctable errors, were made. Fig 15 shows the overlay results with and without additional compensation. Based on predictions, overlay error can be reduced by 3µm or more.

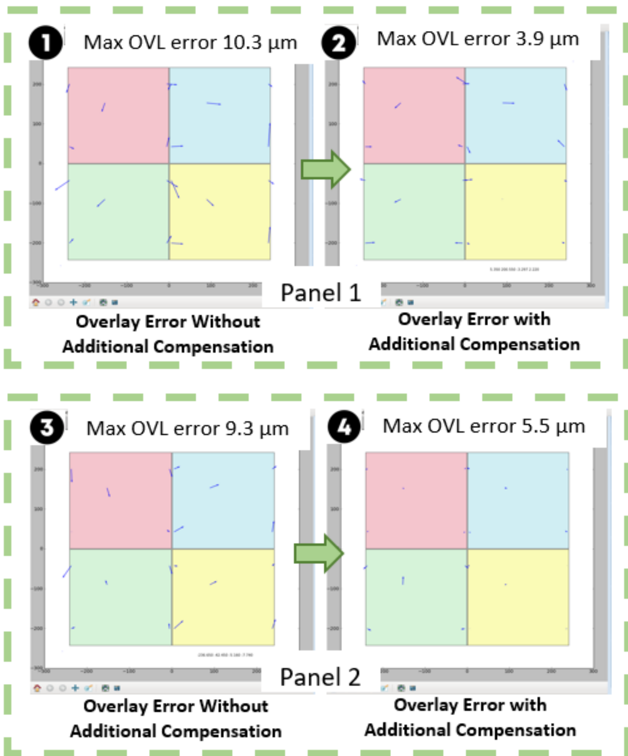

Fig 15. The overlay error with and without additional zone compensation: ① Panel 1 overlay error data without additional compensation: the maximum error vector is 10.3µm.② Panel 1 predicting overlay error with additional compensation: the maximum error vector is 3.9µm. ③ Panel 2 overlay error without additional compensation: the maximum error vector is 9.3µm. ④ Panel 2 overlay error with additional compensation: the maximum error vector is 5.5µm. The prediction results indicate additional compensation can reduce overlay error.

- **Overlay Yield Discussion**

Due to heterogeneous integration and high-performance requirements, resolution will be down to 1µm in advanced packaging and 3µm in AICS in the next few years. In addition, the budget for overlay is getting tighter due to the fine resolution process. In AICS, the typical overlay yield is about 95% to 97% per layer, according to Table 1. A 97% yield threshold is selected for lithography process; this means a 3% yield loss per layer. With six (6) layers in packaging, a 16.7% yield loss can be expected. With an improved yield of 1%, a yield improvement of 5.29% can be expected.

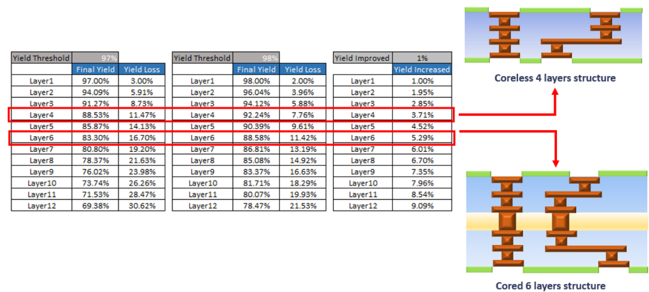

Yield Threshold	97%	
	Final Yield	Yield Loss
Layer1	97.00%	3.00%
Layer2	94.09%	5.91%
Layer3	91.27%	8.73%
Layer4	88.53%	11.47%
Layer5	85.87%	14.13%
Layer6	83.30%	16.70%
Layer7	80.80%	19.20%
Layer8	78.37%	21.63%
Layer9	76.02%	23.98%
Layer10	73.74%	26.26%
Layer11	71.53%	28.47%
Layer12	69.38%	30.62%

Yield Threshold	98%	
	Final Yield	Yield Loss
Layer1	98.00%	2.00%
Layer2	96.04%	3.96%
Layer3	94.12%	5.88%
Layer4	92.24%	7.76%
Layer5	90.39%	9.61%
Layer6	88.58%	11.42%
Layer7	86.81%	13.19%
Layer8	85.08%	14.92%
Layer9	83.37%	16.63%
Layer10	81.71%	18.29%
Layer11	80.07%	19.93%
Layer12	78.47%	21.53%

Yield Improved	1%
	Yield Increased
Layer1	1.00%
Layer2	1.95%
Layer3	2.85%
Layer4	3.71%
Layer5	4.52%
Layer6	5.29%
Layer7	6.01%
Layer8	6.70%
Layer9	7.35%
Layer10	7.96%
Layer11	8.54%
Layer12	9.09%

Table1. Overlay yield table. In this table, the original yield threshold is set to 97%. The final yield loss is 16.7% with six (6) layers of packaging; yield then improved to 98%. The final yield loss is 11.42%, with a 1% improvement to yield; final yield increased 5.29%. The right figures are the examples of six (6) layers packaging and four (4) layer packaging.

IV. Conclusion

This study indicates that an extremely large exposure field fine-resolution lithography system can achieve 3µm resolution and is able to achieve a mean overlay of +3 sigma less than 1µm. It also indicates that an extremely large exposure field fine-resolution lithography system can successfully identify error terms and distortion components in a 510mm x 515mm CCL+ABF stacked panel and correct these to achieve good overlay. According to the analysis and discussion in this study, we understand that proper error and distortion corrections, zone solution correction and additional compensation are key to achieving the best overlay numbers in FOPLP.

In the next few years, with resolution becoming smaller and overlay budgets growing tighter, overlay control will become more important in AICS and advanced packaging.

This study provides users with a path to achieve aggressive overlay requirements.

ACKNOWLEDGEMENT

The authors would like to thank David Giroux, John Kennedy and Karie Li for their work on the software algorithm; Casey Donaher and Perry Banks on the integration work and technical support; Paul Sun and Jeremy Zhang for their work on the lithography processes; and all the team members of the JetStep X500 project.

REFERENCES

[1] John Chang, Onto Innovation, Chip Scale Review November December 2021 Volume 25, Number 6, Large-field, fine-resolution lithography enables next-generation panel-level packaging.
[2] John Chang, Timothy Chang, Casey Donaher, Perry Banks, Aries Peng, Onto Innovation, ECTC2021, Extremely Large Exposure Field with Fine Resolution Lithography Technology to Enable Next Generation Panel Level Advanced Packaging.
[3] Yoshio Nishimura, Ajinomoto Co., Inc., ECTC2019, advanced Insulating Film for Next-Generation Smartphone Performance Requirements
[4] Keith Best, John Chang, Mike Marshall, Jian Lu, Rudolph Technologies IWLPC, 2019, FOPLP lithography solutions to overcome die placement error, predict yield, increase throughput, and reduce cost.
[5] Roger McCleary, Philippe Cochet, Tom Swarbrick, Chin Tiong Sim Rudolph Technologies, Yong Chang Bum, Andy KyawOo, Aung, STATS ChipPAC Singapore, ECTC 2015, Panel Level Advanced Packaging.
[6] James E Webb, Steven Gardner and Elvino DaSilveira, Rudolph Technologies, IMAPS2013, Improved compensation for a reduction stepper to meet the challenges for advanced packaging applications.
[7] Chris Mack, Fundamental Principles of Optical Lithography P.314 – P.326.
[8] John D. Armtiage Jr., Joseph P. Krik, Analysis of overlay distortion patterns.